

Research Article

A Memristor-Based Hyperchaotic System with Hidden Attractors: Dynamics, Synchronization and Circuitual Emulating

V.-T. Pham^{*,1}, Ch. K. Volos², S. Vaidyanathan³, T. P. Le⁴ and V. Y. Vu¹

¹School of Electronics and Telecommunication, Hanoi University of Science and Technology, 01 Dai Co Viet, Hanoi, Vietnam.

²Department of Physics, Aristotle University of Thessaloniki, Thessaloniki, GR-54124, Greece.

³Research and Development Centre, Vel Tech University, Avadi, Chennai-600062, Tamil Nadu, India.

⁴Department of Industrial Management, Ghent University, Belgium.

Received 25 September 2014; Revised 18 October 2014; Accepted 1 November 2014

Abstract

Memristor-based systems and their potential applications, in which memristor is both a nonlinear element and a memory element, have been received significant attention recently. A memristor-based hyperchaotic system with hidden attractor is studied in this paper. The dynamics properties of this hyperchaotic system are discovered through equilibria, Lyapunov exponents, bifurcation diagram, Poincaré map and limit cycles. In addition, its anti-synchronization scheme via adaptive control method is also designed and MATLAB simulations are shown. Finally, an electronic circuit emulating the memristor-based hyperchaotic system has been designed using off-the-shelf components.

Keywords: Memristor, hidden attractor, chaos, synchronization, circuit.

1. Introduction

Three attractive inventions of Professor Leon O. Chua: the Chua's circuit [1], the Cellular Neural/Nonlinear Networks (CNNs) [2,3], and the memristor [4,5] are considered as the major breakthroughs in the literature of the nonlinear science. While Chua's circuit and CNNs have studied and applied in various areas, such as secure communications, random generators, signal processing, pattern formation of modelling of complex systems [6-12], studies on memristor [13-21] have only received significant attention recently after the realization of a solid-state thin film two-terminal memristor at Hewlett-Packard Laboratories [22].

Memristor was proposed by L.O. Chua as the fourth basic circuit element beside the three conventional ones (the resistor, the inductor and the capacitor) [4,23]. Memristor presents the relationship between two fundamental circuit variables, the charge (q) and the flux (φ). Hence, there are two kinds of memristor: charge-controlled memristor and flux-controlled memristor. A charge-controlled memristor is described by

$$v_M = M(q)i_M \quad (1)$$

where v_M is the voltage across the memristor and i_M is the

current through the memristor. Here the memristance (M) is defined by

$$M(q) = \frac{d\varphi(q)}{dq} \quad (2)$$

while the flux-controlled memristor is given by

$$i_M = W(\varphi)v_M \quad (3)$$

where $W(\varphi)$ is the memductance, which is defined by

$$W(\varphi) = \frac{dq(\varphi)}{d\varphi} \quad (4)$$

Moreover, by generalizing the original definition of a memristor [5,23], a memristive system is given as:

$$\begin{cases} \dot{x} = f(x, u, t) \\ y = g(x, u, t)u \end{cases} \quad (5)$$

where u , y , and x denote the input, output and state of the memristive system, respectively. The function f is a continuously differentiable (C^1), n -dimensional vector field and g is a continuous scalar function.

The intrinsic nonlinear characteristic of memristor could be exploited in implementing chaotic systems with complex

* E-mail address: pvt3010@gmail.com

dynamics as well as special features [24,25]. For example, a simple memristor-based chaotic system including only three elements (an inductor, a capacitor and a memristor) was introduced in [26]. Also, a system containing an HP memristor model and triangular wave sequence can generate multi-scroll chaotic attractors [27]. Moreover, a four-dimensional hyperchaotic memristive system with a line equilibrium was also presented by Li [28]. It is worth noting that although a four-dimensional memristive system often only exhibit chaos, the presence of a memristor led Li's system to a hyperchaotic system with hidden attractors.

According to a new classification of chaotic dynamics [29,30], there are two kinds of attractors: *self-excited attractors* and *hidden attractors*. A self-excited attractor has a basin of attraction that is excited from unstable equilibria. As a result, most reported chaotic systems, viz. Lorenz system [31], Rössler system [32], Chen system [33], Sprott system [34], Sundarapandian systems [35-36], Vaidyanathan systems [37-44], Pehlivan system [45], etc., belong to the class of chaotic systems with self-excited attractors. In contrast, a hidden attractor cannot be discovered by using a numerical approach where a trajectory started from a point on the unstable manifold in the neighbourhood of an unstable equilibrium [30,46,47]. Studying systems with hidden attractors is a new research direction because of their practical and theoretical importance [48-53].

In this paper, a memristor-based system without equilibrium is studied. The rest of the paper is organized as follows. In the next Section, the model of the memristor-based system is described. The dynamics and qualitative properties of the memristor-based system are described in Section 3. In Section 4, an anti-synchronization scheme for the identical memristor-based systems is derived via adaptive control theory. In Section 5, circuit implementation of the memristor-based system is studied detail. Finally, the conclusion remarks are drawn in Section 6.

2. Model of Memristor-Based System

In this work, a flux-controlled memristor is used. Similar to other published papers [54-56], its memductance is given as:

$$W(\varphi) = 1 + 6\varphi^2 \tag{6}$$

Based on this memristor, a four-dimensional system is introduced as follows:

$$\begin{cases} \dot{x} = -10x - 5y - 5yz \\ \dot{y} = -6x + 6xz + ayW(\varphi) + b \\ \dot{z} = -z - 6xy \\ \dot{\varphi} = y \end{cases} \tag{7}$$

where a, b are real parameters, and $W(\varphi)$ is the memductance as defined in (6).

When $b = 0$, the memristor-based system (7) has the line equilibrium $E(0, 0, 0, \varphi)$. Interestingly, system (7) is hyperchaotic for different values of the parameter a [28]. For instance, when $a = 0.1, b = 0$ and the selected initial conditions are $(x(0), y(0), z(0), \varphi(0)) = (0, 0.01, 0.01, 0)$, hyperchaos is observed. In this case, memristor-based system (7) is similar to the reported system in [28], hence it will not be discussed in next sections.

3. Dynamics of the Memristor-Based System

We consider the memristor-based system (7) when $b \neq 0$. It is easy to derive the equilibrium for system (7) by solving $\dot{x} = 0, \dot{y} = 0, \dot{z} = 0$, and $\dot{\varphi} = 0$, that is

$$-10x - 5y - 5yz = 0 \tag{8}$$

$$-6x + 6xz + ay(1 + 6\varphi^2) + b = 0 \tag{9}$$

$$-z - 6xy = 0 \tag{10}$$

$$y = 0 \tag{11}$$

Solving (8), (10) and (11), we get $x = y = z = 0$. Thus, Eq. (9) reduces to $b = 0$, which is a contradiction. Hence there is no equilibrium for the memristor-based system (7).

When $a = 0.1, b = -0.001$ and the selected initial conditions are $(x(0), y(0), z(0), \varphi(0)) = (0, 0.01, 0.01, 0)$, the Lyapunov exponents of the system (7) are $\lambda_1 = 0.1244, \lambda_2 = 0.0136, \lambda_3 = 0$ and $\lambda_4 = -10.8161$. Thus, the memristor-based system (7) is a hyperchaotic system because it has more than one positive Lyapunov exponents [57]. Moreover, this memristor-based system can be classified as a hyperchaotic system with hidden strange attractor, a basin of attraction of which does not contain neighbourhoods of equilibria [30,58]. To the best of our knowledge there are only few works reporting hyperchaotic hidden strange attractor [28,50,59]. It is noting that system (7) has been proposed briefly in [59], but the behavior of such a system has not been investigated. The projections of the hyperchaotic attractor without equilibrium for this set of parameters are shown in Fig. 1.

The Kaplan-Yorke fractional dimension, that presents the complexity of attractor [60], is defined by

$$D_{KY} = j + \frac{1}{|\lambda_{j+1}|} \sum_{i=1}^j \lambda_i \tag{12}$$

where j is the largest integer satisfying $\sum_{i=1}^j \lambda_i \geq 0$ and

$$\sum_{i=1}^{j+1} \lambda_i < 0.$$

The calculated fractional dimension of memristor-based system (7) when $a = 0.1, b = -0.001$ is $D_{KY} = 3.0128 > 3$. Thus, it indicates a strange attractor. Moreover, as it can be seen from the Poincaré map (Fig. 2), memristor-based system (7) exhibits a rich dynamical behavior.

It is worth mentioning that Lyapunov exponents measure the exponential rates of the divergence and convergence of nearby trajectories in the phase space of the chaotic system [6,33] and for a four-dimension hyperchaotic system there are two positive Lyapunov exponents, one zero, and one negative Lyapunov exponent. Thus Lyapunov exponents of memristor-based system (7) have been calculated using well-known algorithm in [61] to verify its hyperchaos.

In our work, the parameter b is fixed as $b = -0.001$, while the parameter a indicating the strength of the memristor is varied. The bifurcation diagram is presented in Fig. 3 by plotting the local maxima of the state variable $z(t)$ when changing the value of the parameter a . The spectrum of the corresponding Lyapunov exponents is depicted in Fig. 4.

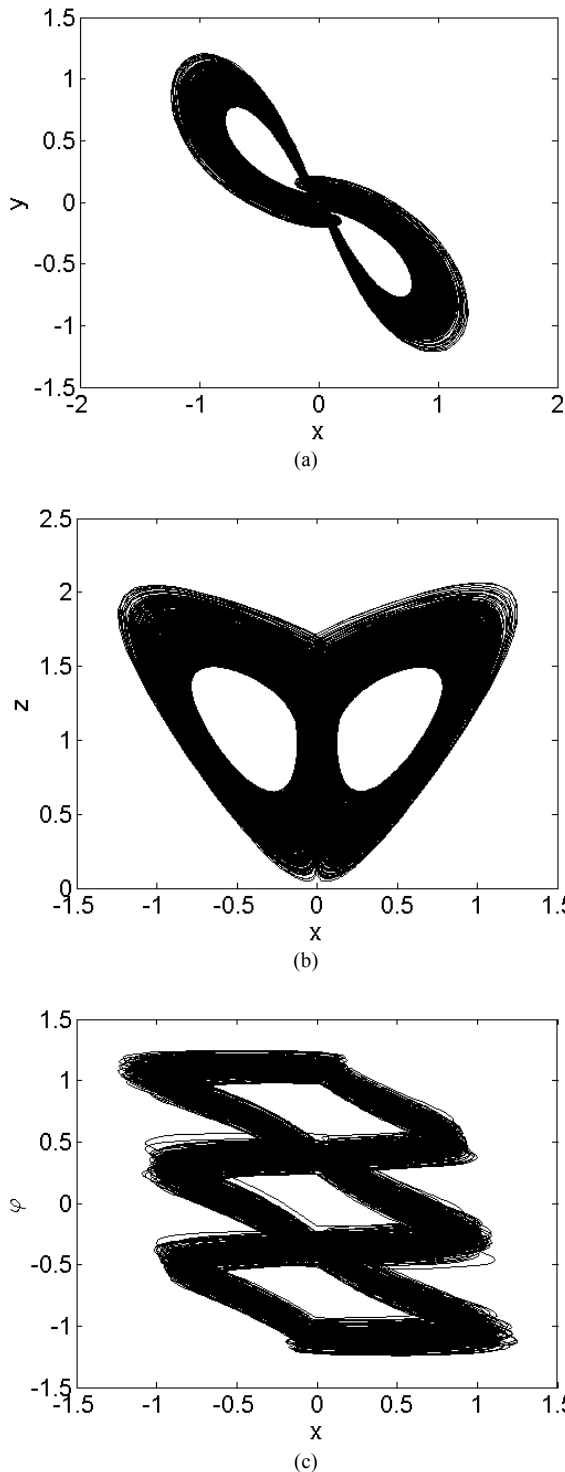


Fig. 1. The projection of the hyperchaotic attractor of memristor-based system (7) for $a = 0.1$, and $b = -0.001$ (a) in the x - y phase plane, (b) in the x - z phase plane and (c) in the x - ϕ phase plane.

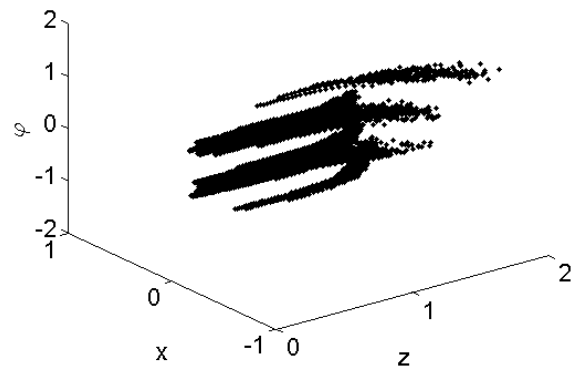


Fig. 2. Poincaré map in the x - z - ϕ space plane when $y = 0$ for $a = 0.1$, and $b = -0.001$.

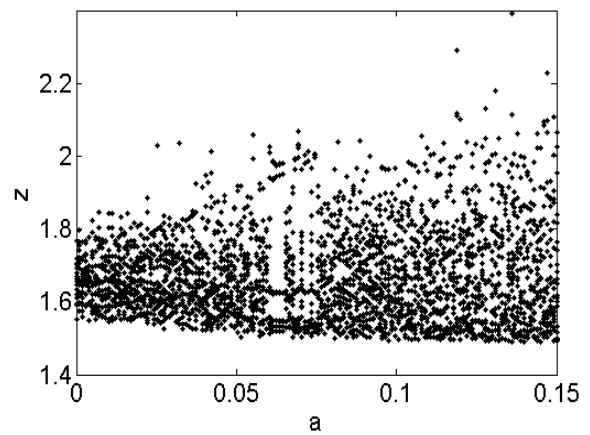


Fig. 3. Bifurcation diagram of z_{\max} with $b = -0.001$ and a as varying parameter.

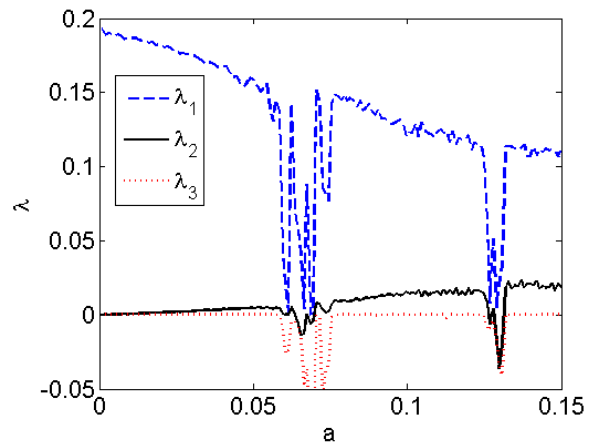


Fig. 4. Three largest Lyapunov exponents of memristor-based system (7) versus a for $b = -0.001$.

Lyapunov exponents reported in Fig. 4 agree well with the bifurcation diagram of Fig. 3. As shown in Figs. 3 and 4, there are some windows of limits cycles, of chaotic behavior and of hyperchaotic behavior. For example, the periodic orbit of memristor-based system (7) for the parameter $a = 0.07$ is illustrated in Fig. 5.

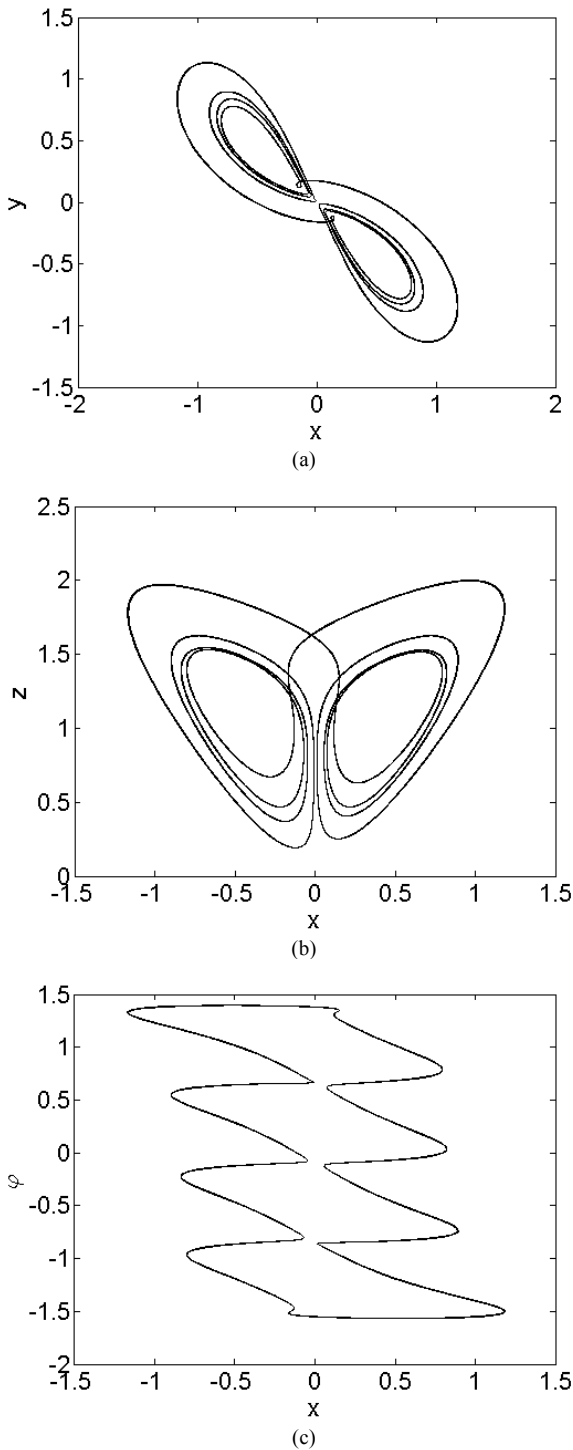


Fig. 5. The periodic orbit of memristor-based system (7), for $a = 0.07$, and $b = -0.001$ (a) in the x - y phase plane, (b) in the x - z phase plane and (c) in the x - ϕ phase plane.

4. Adaptive Anti-Synchronization of Identical Memristor-Based Systems

The study of anti-synchronization of chaotic systems is an important research problem in the chaos literature [62-65].

The anti-synchronization of chaotic systems involves a pair of chaotic systems called the master or drive system and slave or response systems, and the design problem is to find an effective feedback control law so that the outputs of the master and slave systems are equal in magnitude and

opposite in sign asymptotically. In other words, when anti-synchronization is achieved between the master and slave chaotic systems, the sum of the outputs of the two systems will converge to zero asymptotically with time.

This section will present the adaptive anti-synchronization of identical memristor-based hyperchaotic systems with unknown parameters a and b . We use estimates $A(t)$ and $B(t)$ for the unknown parameters a and b , respectively.

Adaptive control method is used to derive update laws for the parameter estimates and Lyapunov stability theory is used to establish the main anti-synchronization result of this section. Adaptive control method is known to be an effective method for the synchronization and anti-synchronization of chaotic systems [66-70].

As the master system, we consider the memristor-based system dynamics

$$\begin{cases} \dot{x}_1 = -10x_1 - 5y_1 - 5y_1z_1 \\ \dot{y}_1 = -6x_1 + 6x_1z_1 + ay_1W(\phi_1) + b \\ \dot{z}_1 = -z_1 - 6x_1y_1 \\ \dot{\phi}_1 = y_1 \end{cases} \quad (13)$$

In (13), $W(\phi)$ is the memductance as defined in (6). Also, x_1, y_1, z_1, ϕ_1 are the states of the master system (13).

As the slave system, we consider the controlled memristor-based system dynamics

$$\begin{cases} \dot{x}_2 = -10x_2 - 5y_2 - 5y_2z_2 + u_x \\ \dot{y}_2 = -6x_2 + 6x_2z_2 + ay_2W(\phi_2) + b + u_y \\ \dot{z}_2 = -z_2 - 6x_2y_2 + u_z \\ \dot{\phi}_2 = y_2 + u_\phi \end{cases} \quad (14)$$

Here x_2, y_2, z_2, ϕ_2 are the states of the slave system (14) and u_x, u_y, u_z, u_ϕ are the adaptive controls to be determined for the anti-synchronization of the systems (13) and (14).

The system parameters a and b are unknown and hence, we use estimates $A(t)$ and $B(t)$ for a and b , respectively.

The anti-synchronization error between the memristor-based systems (13) and (14) is defined as follows:

$$\begin{cases} e_x = x_1 + x_2 \\ e_y = y_1 + y_2 \\ e_z = z_1 + z_2 \\ e_\phi = \phi_1 + \phi_2 \end{cases} \quad (15)$$

Thus, the anti-synchronization error dynamics is got as:

$$\begin{cases} \dot{e}_x = -10e_x - 5e_y - 5(y_1z_1 + y_2z_2) + u_x \\ \dot{e}_y = -6e_x + 6(x_1z_1 + x_2z_2) + a[y_1W(\phi_1) + y_2W(\phi_2)] + 2b + u_y \\ \dot{e}_z = -e_z - 6(x_1y_1 + x_2y_2) + u_z \\ \dot{e}_\phi = e_y + u_\phi \end{cases} \quad (16)$$

As an adaptive feedback control law to stabilize the system (16), we take

$$\begin{cases} \dot{u}_x = 10e_x + 5e_y + 5(y_1z_1 + y_2z_2) - k_x e_x \\ \dot{u}_y = 6e_x - 6(x_1z_1 + x_2z_2) + \\ - A(t)[y_1W(\varphi_1) + y_2W(\varphi_2)] - 2B(t) - k_y e_y \\ \dot{u}_z = e_z + 6(x_1y_1 + x_2y_2) - k_z e_z \\ \dot{e}_\varphi = -e_y - k_\varphi e_\varphi \end{cases} \quad (17)$$

In (17), $A(t)$ and $B(t)$ are estimates for the unknown system parameters a and b , respectively. Also, k_x, k_y, k_z and k_φ are assumed to be positive gain constants.

Substituting (17) into (16), we get the closed-loop error dynamics as:

$$\begin{cases} \dot{e}_x = -k_x e_x \\ \dot{e}_y = (a - A(t))[y_1W(\varphi_1) + y_2W(\varphi_2)] + \\ + 2(b - B(t)) - k_y e_y \\ \dot{e}_z = -k_z e_z \\ \dot{e}_\varphi = -k_\varphi e_\varphi \end{cases} \quad (18)$$

We define the parameter estimation errors as:

$$\begin{cases} e_a(t) = a - A(t) \\ e_b(t) = b - B(t) \end{cases} \quad (19)$$

Differentiating (19) with respect to t , we get

$$\begin{cases} \dot{e}_a(t) = -\dot{A}(t) \\ \dot{e}_b(t) = -\dot{B}(t) \end{cases} \quad (20)$$

Substituting (19) into (18), we get the error dynamics as:

$$\begin{cases} \dot{e}_x = -k_x e_x \\ \dot{e}_y = e_a[y_1W(\varphi_1) + y_2W(\varphi_2)] + 2e_b - k_y e_y \\ \dot{e}_z = -k_z e_z \\ \dot{e}_\varphi = -k_\varphi e_\varphi \end{cases} \quad (21)$$

We consider the quadratic Lyapunov function

$$V = \frac{1}{2}(e_x^2 + e_y^2 + e_z^2 + e_a^2 + e_b^2) \quad (22)$$

Clearly, V is a positive definite function on R^6 .

Differentiating V along the trajectories of (18) and (20), we get

$$\begin{aligned} \dot{V} = & -k_x e_x^2 - k_y e_y^2 - k_z e_z^2 - k_\varphi e_\varphi^2 + \\ & + e_a [e_y [y_1W(\varphi_1) + y_2W(\varphi_2)] - \dot{A}] + \\ & + e_b [2e_y - \dot{B}] \end{aligned} \quad (23)$$

In view of (23), we define an update law for the parameter estimates as:

$$\begin{cases} \dot{A} = e_y [y_1W(\varphi_1) + y_2W(\varphi_2)] \\ \dot{B} = 2e_y \end{cases} \quad (24)$$

Theorem 1. *The identical memristor-based systems (13) and (14) with unknown parameters a and b are exponentially and globally anti-synchronized by the adaptive control law (17) and the parameter update law (24), where the gain constants k_x, k_y, k_z, k_φ are positive and $A(t), B(t)$ are estimates for a and b , respectively.*

Proof. The result is proved via Lyapunov stability theory. For this purpose, we consider the quadratic Lyapunov function V defined by (22), which is positive definite on R^6 .

Substituting the parameter update law (24) into (23), we obtain \dot{V} as:

$$\dot{V} = -k_x e_x^2 - k_y e_y^2 - k_z e_z^2 - k_\varphi e_\varphi^2 \quad (25)$$

Clearly, \dot{V} is a negative semi-definite function on R^6 .

Thus, we can conclude that the anti-synchronization error $e(t)$ and the parameter estimation error $[e_a(t) \ e_b(t)]^T$ are globally bounded.

We define $k = \min\{k_x, k_y, k_z, k_\varphi\}$.

Then it is clear from (25) that

$$\dot{V} \leq -k \|e\|^2 \text{ or } k \|e\|^2 \leq -\dot{V} \quad (26)$$

Integrating the inequality (26) from 0 to t , we get

$$k \int_0^t \|e(\tau)\|^2 d\tau \leq -\int_0^t \dot{V}(\tau) d\tau = V(0) - V(t) \quad (27)$$

Therefore, we can conclude that $e(t) \in L_2$.

Using (21), we can conclude that $\dot{e}(t) \in L_2$.

Using Barbalat's lemma [71], $e(t) \rightarrow 0$ exponentially as $t \rightarrow \infty$ for all initial conditions $e(0) \in R^4$. ■

For numerical simulations, the classical fourth-order Runge-Kutta method with step size $h = 10^{-8}$ is used to solve the systems of differential equations (13), (14) and (24), when the adaptive control law (17) is applied.

The parameter values of the memristor system are taken as in the hyperchaotic case, viz. $a = 0.07$ and $b = -0.001$.

The gain constants are taken as: $k_x = k_y = k_z = k_\varphi = 5$. As initial conditions of the master system (13), we take $x_1(0) = 7.4, y_1(0) = -3.5, z_1(0) = 3.4, \varphi_1(0) = -1.7$, while as initial conditions of the slave system (14), we take $x_2(0) = 4.3, y_2(0) = -1.2, z_2(0) = 2.8, \varphi_2(0) = -2.4$. Furthermore, as initial conditions of the estimates $A(t)$ and $B(t)$, we take $A(0) = 1.2$ and $B(0) = 2.5$.

In Figs. 6-9, the anti-synchronization of the states of the master system (13) and the slave system (14) is depicted. Fig. 6 depicts the anti-synchronization of the states x_1 and x_2 of the systems (13) and (14). Fig. 7 depicts the anti-synchronization of the states y_1 and y_2 of the systems (13) and (14). Fig. 8 depicts the anti-synchronization of the states z_1 and z_2 of the systems (13) and (14). Fig. 8 depicts the anti-synchronization of the states φ_1 and φ_2 of the systems (13) and (14). In Fig. 10, the time-history of the anti-synchronization errors $e_x(t), e_y(t), e_z(t), e_\varphi(t)$ is depicted.

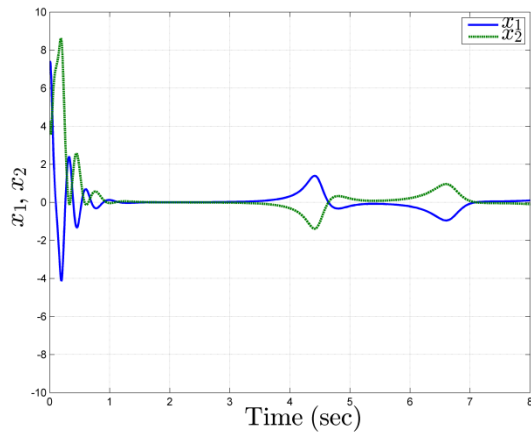


Fig. 6. Anti-synchronization of the states x_1 and x_2 .

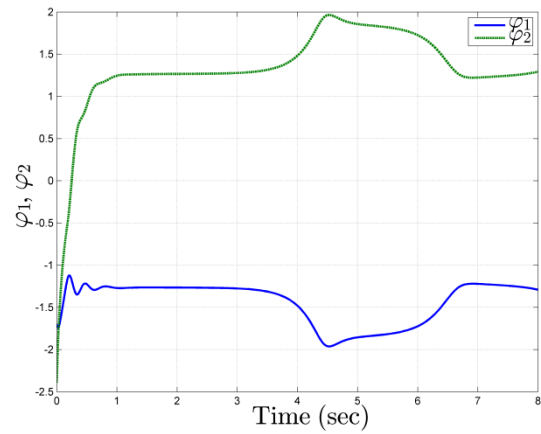


Fig. 9. Anti-synchronization of the states φ_1 and φ_2 .

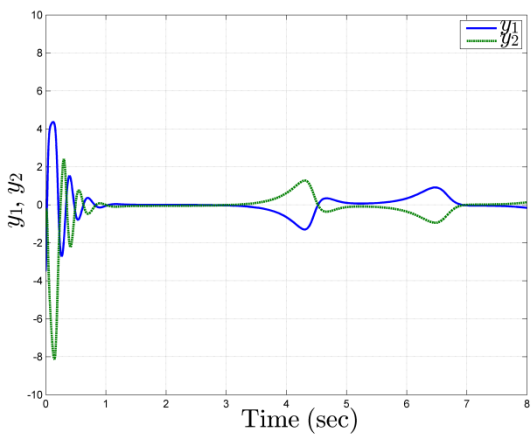


Fig. 7. Anti-synchronization of the states y_1 and y_2 .

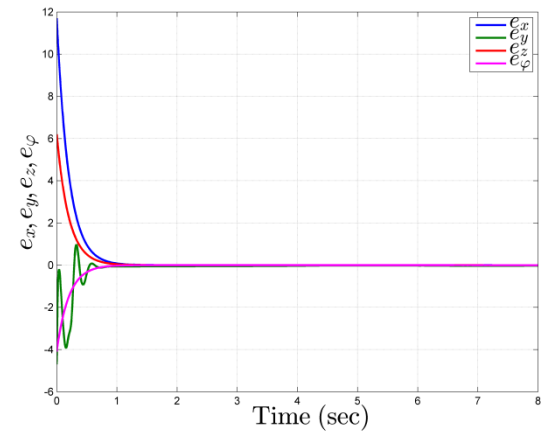


Fig. 10. Time-history of the anti-synchronization errors.

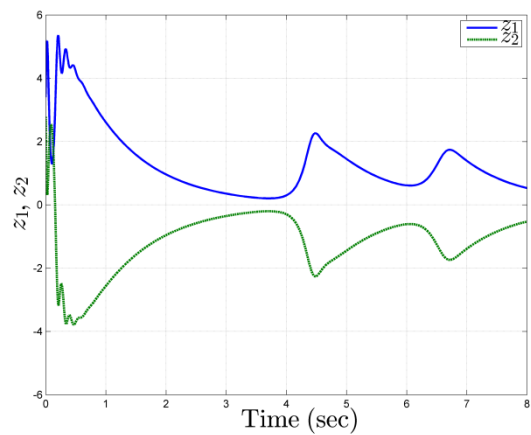


Fig. 8. Anti-synchronization of the states z_1 and z_2 .

5. Circuitual Design of the Memristor-Based System

Using electronic circuits emulating chaotic/hyperchaotic systems is an effective approach for investigating dynamics of such systems [6,7,72]. Some advantages of this physical approach can be listed as avoiding the uncertainties arising from systematic and statistical errors in numerical simulations, reducing long simulation time or displaying attractors on the oscilloscope easily [7,73]. From the point of view of practical applications, the realization of chaotic electronic circuits based on theoretical models is a vital topic. Such circuits are main parts in diverse chaos-based applications such as image encryption scheme, path planning generator for autonomous mobile robots, or random bit generator [74-80].

In this Section, an electronic circuit is designed to implement memristor-based system (7). The circuit in Fig. 11 has been designed following a general approach based on operational amplifiers [7]. The variables x, y, z, φ of system (7) are the voltages across the capacitor $C_1, C_2, C_3,$ and $C_4,$ respectively. As shown in Fig. 11 the memristor is realized by common electronic components. Indeed the sub-circuit of memristor in Fig. 11 only emulates the memristor because there are not any commercial off-the-shelf memristors in the market yet. By applying Kirchhoff's circuit laws, the corresponding circuitual equations of circuit can be written as:

$$\begin{cases} \frac{dv_{C_1}}{dt} = -\frac{1}{R_1 C_1} v_{C_1} - \frac{1}{R_2 C_1} v_{C_2} - \frac{1}{10 R_3 C_1} v_{C_2} v_{C_3} \\ \frac{dv_{C_2}}{dt} = -\frac{1}{R_4 C_2} v_{C_1} + \frac{1}{10 R_5 C_2} v_{C_1} v_{C_3} - \frac{1}{R_7 C_2} V_b + \\ \quad + \frac{1}{R_6 C_2} v_{C_2} \left(\frac{R_{11}}{R_{12}} + \frac{R_{11}}{100 R_{13}} v_{C_4}^2 \right) \\ \frac{dv_{C_3}}{dt} = -\frac{1}{R_8 C_3} v_{C_3} - \frac{1}{10 R_9 C_3} v_{C_1} v_{C_2} \\ \frac{dv_{C_4}}{dt} = \frac{1}{R_{10} C_4} v_{C_2} \end{cases} \quad (28)$$

where, $a = \frac{1}{R_6 C_2}$ and $b = \frac{1}{R_7 C_2} V_b$.

The operational amplifiers in this paper's circuit are TL084 ones, of which power supplies are ± 15 Volts. We set the values of components as follows: $R_1 = R_3 = 1.8 \text{ k}\Omega$, $R_2 = 3.6 \text{ k}\Omega$, $R_4 = 3 \text{ k}\Omega$, $R_5 = R_9 = 1.5 \text{ k}\Omega$, $R_6 = 180 \text{ k}\Omega$, $R_7 = 90 \text{ k}\Omega$, $R_8 = R_{10} = R_{11} = R_{12} = R = 18 \text{ k}\Omega$, $R_{13} = 0.75 \text{ k}\Omega$, $C_1 = C_2 = C_3 = C_4 = 10 \text{ nF}$, and $V_b = 1 \text{ mV}_{DC}$.

The design circuit is implemented in the electronic simulation package Multisim. Obtained results are presented in Figs. 12 & 13. Obviously, theoretical attractors (see Fig. 1) look similar with the circuitual ones shown in Fig. 12. In order to investigate the dynamics of the designed memristor-based circuit in Fig.11 with respect to the strength of the memristor, the value of resistor R_6 can be varied by using a trimmer. For instance, when $R_6 = 257.14 \text{ k}\Omega$ the behavior of the circuit is a periodic limit cycle (see Fig. 13) corresponding to an implemented value of $a = 0.07$, which can be compared to the model behavior reported in Fig. 5

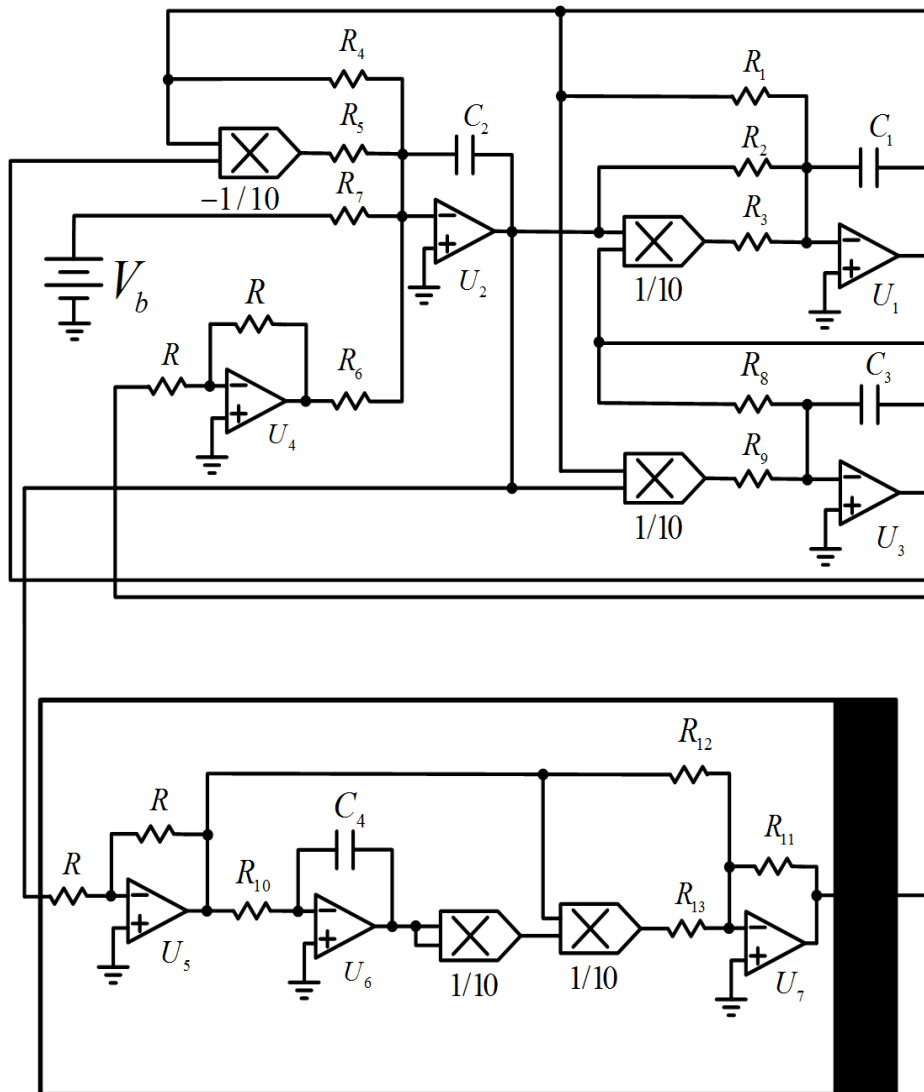
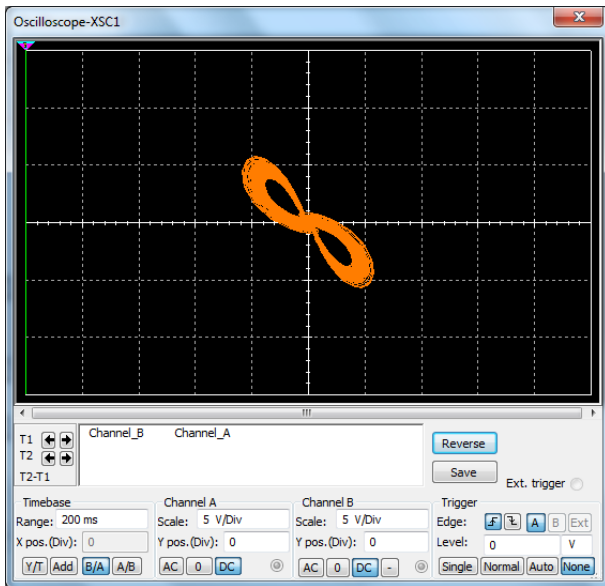
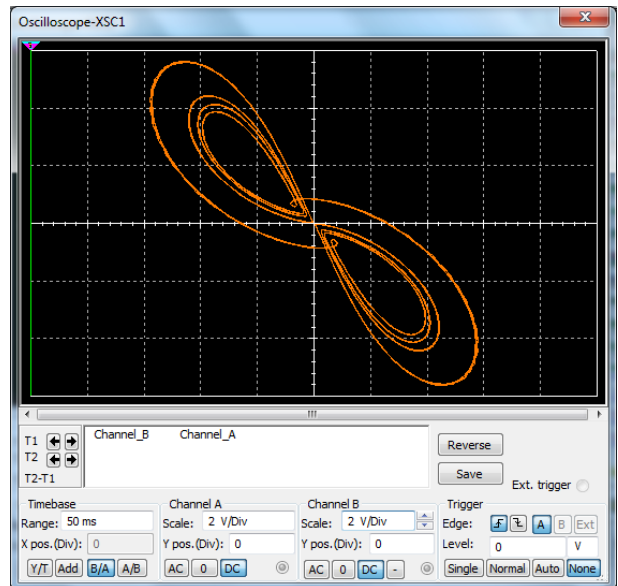


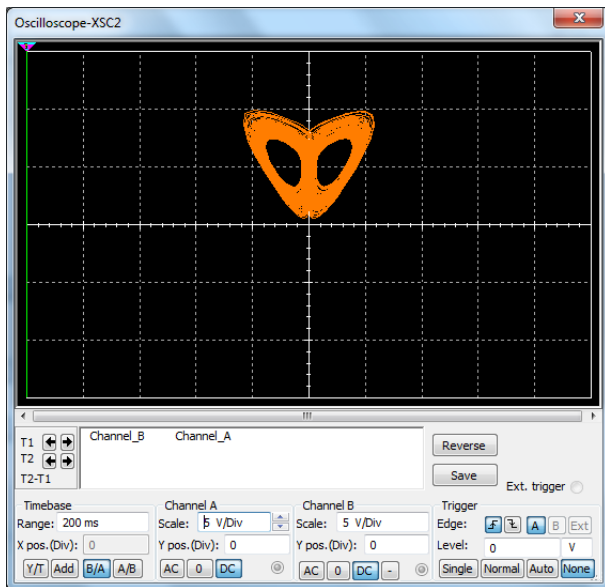
Fig 11. Schematic of the circuit which emulating memristor-based system (7).



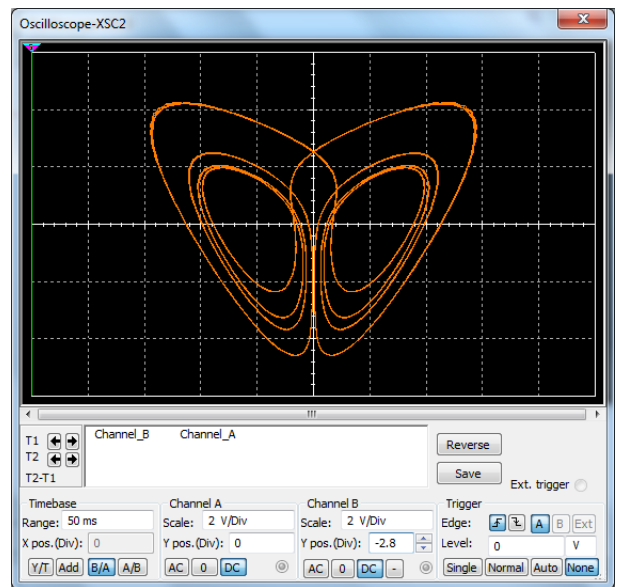
(a)



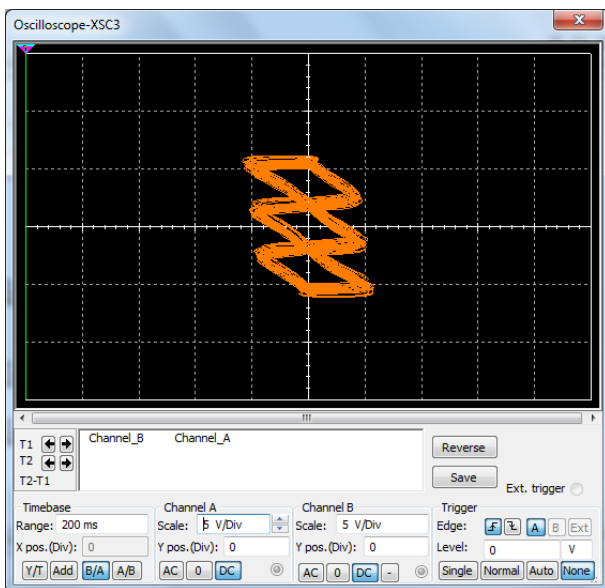
(a)



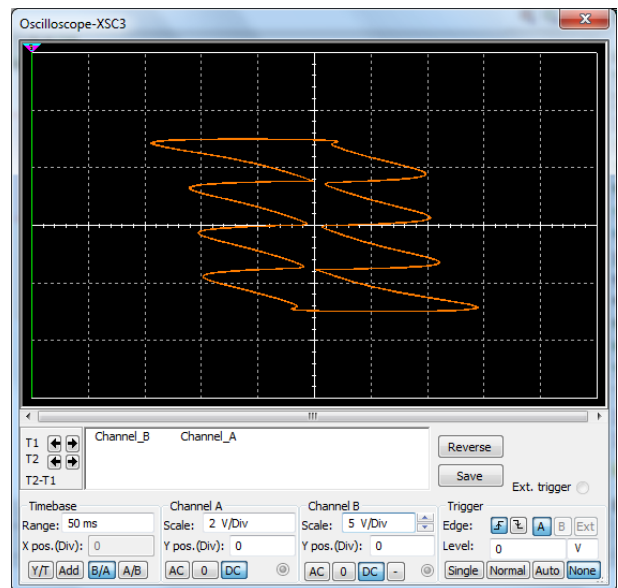
(b)



(b)



(c)



(c)

Fig. 12. Hyperchaotic attractor of the designed circuit obtained from Multisim (a) in the v_{C1} - v_{C2} phase plane, (b) in the v_{C1} - v_{C3} phase plane and (c) in the v_{C1} - v_{C4} phase plane.

Fig. 13. Periodic orbit of the designed circuit obtained from Multisim, for $a = 0.07$ and $b = -0.001$, (a) in the v_{C1} - v_{C2} phase plane, (b) in the v_{C1} - v_{C3} phase plane and (c) in the v_{C1} - v_{C4} phase plane.

6. Conclusion

In this paper, a memristor-based system has been studied. This memristor-based system displays rich dynamical behavior as confirmed by numerical simulations and circuit implementation. Moreover, the possibility of anti-synchronization scheme of memristor-based systems has been designed via adaptive control method and MATLAB simulations are shown to illustrate the anti-synchronization results. It is worth noting that the presence of the memristor creates some special and unusual features. For example, such memristor-based systems can exhibit chaos although it possesses no equilibrium points. We have shown that our memristor-based system can exhibit hyperchaotic attractors.

It is well known that hyperchaotic system, which is characterized by more than one positive Lyapunov exponent, presents a higher level of complexity with respect to a conventional chaotic system. Hence, we can apply this memristor-based hyperchaotic system in practical applications like cryptosystems, encryption, neural networks and secure communications.

Acknowledgements

This research is funded by Vietnam National Foundation for Science and Technology Development (NAFOSTED) under grant number 102.99-2013.06.

References

1. T. Matsumoto, A Chaotic attractor from Chua's circuit, *IEEE Trans. Circuits Sys.*, vol. 31, pp. 1055-1058 (1984).
2. L.O. Chua and L. Yang, Cellular neural networks: Theory, *IEEE Trans. Circuits Sys.*, vol. 35, pp. 1257-1272 (1988).
3. L.O. Chua and L. Yang, Cellular neural networks: Applications, *IEEE Trans. Circuits Sys.*, vol. 35, pp. 1273-1290 (1988).
4. L.O. Chua, Memristor - the missing circuit element, *IEEE Transactions on Circuit Theory*, vol. 18(5), pp. 507-519 (1971).
5. L.O. Chua and S.M. Kang, Memristive devices and systems, In *Proceedings of the IEEE*, vol. 64, pp. 209-223 (1976).
6. S. H. Strogatz, *Nonlinear dynamics and chaos: With applications to physics, biology, chemistry, and engineering*, Perseus Books, Massachusetts, USA (1994).
7. L. Fortuna, M. Frasca and M.G. Xibilia, Chua's circuit implementations: Yesterday, today and tomorrow, *World Scientific*, Singapore (2009).
8. L.O. Chua, Chua's circuit: An overview ten years later, *J. Circuit Sys. Computer*, vol. 4, pp. 117-159 (1994).
9. L.O. Chua, *CNN: A paradigm for complexity*, World Scientific, Singapore (1998).
10. P. Arena, M. Bucolo, S. Fazzino, L. Fortuna, and M. Frasca, The CNN paradigm: Shapes and complexity, *Int. J. Bif. Chaos*, vol. 7, 2063-2090 (2005).
11. L.O. Chua and T. Roska, *Cellular neural networks and visual computing*, Cambridge University Press, Cambridge, UK (2002).
12. V. Perez-Munuzuri, V. Perez-Villar, and L.O. Chua, Autowaves for image processing on a two-dimensional CNN array of excitable nonlinear circuits: Flat and wrinkled labyrinths, *IEEE Trans. Circuits Sys. I: Fund, Theory Appl.*, vol. 40, pp. 174-181 (1993).
13. Y.N. Joglekar and S.J. Wolf, The elusive memristor: Properties of basic electrical circuits, *European Journal of Physics*, vol. 30, pp. 661-675 (2009).
14. Y.V. Pershin and M. Di Ventra, Experimental demonstration of associative memory with memristive neural networks, *Neural Networks*, vol. 23, p. 881 (2010).
15. T. Driscoll, J. Quinn, S. Klein, H. T. Kim, B. J. Kim, Y.V. Pershin, M. Di Ventra, and D.N. Basov, Memristive adaptive filters, *Appl. Phys. Lett.*, vol. 97, pp. 093502 (2010).
16. S. Shin, K. Kim, and S. M. Kang, Memristor applications for programmable analog ICs, *IEEE Trans. Nanotechnology*, vol. 410, pp. 266-274 (2011).
17. L. Wang, Ch. Zhang, L. Chen, J. Lai, and J. Tong, A novel memristor-based 1SRAM structure for multiple-bit upsets immunity, *IEICE Electronics Express*, vol. 9, pp. 861-867 (2012).
18. Y. Shang, W. Fei, and H. Yu, Analysis and modeling of internal state variables for dynamic effects of nonvolatile memory devices, *IEEE Trans. Circuits Sys. I: Regular Papers*, vol. 59, pp. 1906-1918 (2012).
19. S.P. Adhikari, C. Yang, H. Kim, and L.O. Chua, Memristor bridge synapse-based neural network and its learning, *IEEE Transactions on Neural Networks and Learning Systems*, vol. 23, pp. 1426-1435 (2012).
20. S.P. Adhikari, M.P. Sad, H. Kim, and L.O. Chua, Three fingerprints of memristor, *IEEE Trans. Circuits Sys. I: Regular Papers*, vol. 60, pp. 3008-3021 (2013).
21. J.J. Yang, D.B. Strukov, and D.R. Stewart, Memristive devices for computing, *Nature Nanotechnology*, vol. 8, pp. 13-24 (2013).
22. D. Strukov, G. Snider, G. Stewart, and R. Williams, The missing memristor found, *Nature*, vol. 453, pp. 80-83 (2008).
23. R. Tetzlaff, *Memristors and resistive systems*, Springer, New York, USA (2014).
24. M. Itoh and L.O. Chua, Memristor oscillators, *Int. J. Bif. Chaos*, vol. 18, pp. 3183-3206 (2008).
25. M. Muthuswamy, Memristor based chaotic circuits, *IETE Tech. Rep.*, vol. 26, pp. 417-429 (2009).
26. B. Muthuswamy and L.O. Chua, Simplest chaotic circuit, *Int. J. Bif. Chaos*, vol. 20, pp. 1567-1580 (2010).
27. H. Li, L. Wang and S. Duan, A memristor-based scroll chaotic system - Design, Analysis and circuit implementation, vol. 24, pp. 1450099 (2014)
28. Q. Li, S. Hu, S. Tang and G. Zeng, Hyperchaos and horseshoe in a 4D memristive system with a line of equilibria and its implementation, *Int. J. Circuit Theory Appl.*, DOI: 10.1002/cta.1912 (2013).
29. G. Leonov, N. Kuznetsov, S. Seldedzhi and V. Vagitsev, Hidden oscillations in dynamical systems. *Trans. Syst. Contr.*, vol. 6, pp. 54-67 (2011).
30. G. Leonov and N. Kuznetsov, Hidden attractors in dynamical systems: From hidden oscillation in Hilbert-Kolmogorov, Aizerman and Kalman problems to hidden chaotic attractor in Chua circuits, *Int. J. Bif. Chaos*, vol. 23, pp. 1330002 (2013)
31. E.N. Lorenz, Deterministic nonperiodic flow, *Journal of the Atmospheric Sciences*, vol. 20, pp. 130-141 (1963).
32. O.E. Rössler, An equation for continuous chaos, *Physics Letters A*, vol. 57, pp. 397-398 (1976).
33. G. Chen and T. Ueta, Yet another chaotic attractor, *International Journal of Bifurcation and Chaos*, vol. 9, pp. 1465-1466 (1999).
34. J.C. Sprott, Some simple chaotic flows, *Physical Review E*, vol. 50, pp. 647-650 (1994).
35. V. Sundarapandian and I. Pehlivan, Analysis, control, synchronization and circuit design of a novel chaotic system, *Mathematical and Computer Modelling*, vol. 55, pp. 1904-1915 (2012).
36. V. Sundarapandian, Analysis and anti-synchronization of a novel chaotic system via active and adaptive controllers, *Journal of Engineering Science and Technology Review*, vol. 6, pp. 45-52 (2013).
37. S. Vaidyanathan, A new six-term 3-D chaotic system with an exponential nonlinearity, *Far East Journal of Mathematical Sciences*, vol. 79, pp. 135-143 (2013).
38. S. Vaidyanathan, Analysis and adaptive synchronization of two novel chaotic systems with hyperbolic sinusoidal and cosinusoidal nonlinearity and unknown parameters, *Journal of Engineering Science and Technology Review*, vol. 6, pp. 53-65 (2013).

39. S. Vaidyanathan, A new eight-term 3-D polynomial chaotic system with three quadratic nonlinearities, *Far East Journal of Mathematical Sciences*, vol. 84, pp. 219-226 (2014).
40. S. Vaidyanathan, Analysis, control and synchronization of a six-term novel chaotic system with three quadratic nonlinearities, *International Journal of Modelling, Identification and Control*, vol. 22, pp. 41-53 (2014).
41. S. Vaidyanathan, Analysis and adaptive synchronization of eight-term 3-D polynomial chaotic systems with three quadratic nonlinearities, *European Physical Journal: Special Topics*, vol. 223, pp. 1519-1529 (2014).
42. S. Vaidyanathan, A ten-term novel 4-D hyperchaotic system with three quadratic nonlinearities and its control, *International Journal of Control Theory and Applications*, vol. 6(2), pp. 97-109 (2013).
43. S. Vaidyanathan and K. Madhavan, Analysis, adaptive control and synchronization of a seven-term novel 3-D chaotic system, *International Journal of Control Theory and Applications*, vol. 6(2), pp. 121-127 (2013).
44. S. Vaidyanathan, C. Volos, V.-T. Pham, K. Madhavan and B.A. Idowu, Adaptive backstepping control, synchronization and circuit simulation of a 3-D novel jerk chaotic system with two hyperbolic sinusoidal nonlinearities, *Archives of Control Sciences*, vol. 24(3), pp. 257-285 (2014).
45. I. Pehlivan, I.M. Moroz, and S. Vaidyanathan, Analysis, synchronization and circuit design of a novel butterfly attractor, *Journal of Sound and Vibration*, vol. 333, pp. 5077-5096 (2014).
46. G. Leonov, N. Kuznetsov, and V. Vagitsev, Localization of hidden Chua's attractors, *Phys. Lett. A*, vol. 375, pp. 2230-2233 (2011).
47. G. Leonov, N. Kuznetsov, and V. Vagitsev, Hidden attractor in smooth Chua system, *Physica D*, vol. 241, pp. 1482-1486 (2011).
48. M. Molaei, S. Jafari, J.C. Sprott and S. Golpayegani, Simple chaotic flows with no stable equilibrium, *Int. J. Bif. Chaos*, vol. 23, pp. 1350188 (2013).
49. S. Jafari, J.C. Sprott and S. Golpayegani, Elementary quadratic chaotic flows with no equilibria, *Phys. Lett. A*, vol. 377, pp. 699-702 (2013).
50. Z. Wang, S. Cang, E. Ochola and Y. Sun, A hyperchaotic system without equilibrium, *Nonlin. Dyn.*, vol. 69, pp. 531-537 (2012).
51. X. Wang and G. Chen, Constructing a chaotic system with any number of equilibria, *Nonlin. Dyn.*, vol. 71, pp. 429-436 (2013).
52. Z. Wei, Dynamical behaviors of a chaotic system with no equilibria, *Phys. Lett. A*, vol. 376, pp. 102-108 (2011).
53. V.-T. Pham, C. Volos, S. Jafari, Z. Wei and X. Wang, Constructing a novel no-equilibrium chaotic system, *Int. J. Bif. Chaos*, vol. 24, pp. 1450073 (2014).
54. B. Muthuswamy, Implementing memristor based chaotic circuits, *Int. J. Bif. Chao*, vol. 20, pp. 1335-1350 (2010).
55. B.C. Bao, Z. Liu, B.P. Xu, Dynamical analysis of memristor chaotic oscillator, *Acta Physica Sinica*, vol. 59, pp. 3785-3793 (2010).
56. A.L. Fitch, D.S. Yu, H.H.C. Iu and V. Sreeram, Hyperchaos in a memristor-based modified canonical Chua's circuit, *Int. J. Bif. Chao*, vol. 22, pp. 1250133 (2012).
57. O. RöSSLer, An equation for hyperchaos, *Phys. Lett. A*, vol. 71, pp. 155-157 (1979).
58. S. Jafari and J.C. Sprott, Simple chaotic flows with a line equilibrium, *Chaos Solitons Fractals*, vol. 57, pp. 79-84 (2013).
59. V.-T. Pham, C. Volos, S. Jafari, and X. Wang, Generating a novel hyperchaotic system out of equilibrium, *Optoelectron. Adv. Mater. Rapid Comm.*, vol. 8, pp. 535-539 (2014).
60. P. Frederickson, J.L. Kaplan, E.D. Yorke and J.A. York, The Lyapunov dimension of strange attractors. *J. Differential Equations*, vol. 49, pp. 185-207 (1983).
61. A. Wolf, J.B. Swift, H.L. Swinney and J.A. Vastano, Determining Lyapunov exponents from a time series, *Physica D*, vol. 16, pp. 285-317 (1985).
62. S. Vaidyanathan and S. Sampath, Anti-synchronization of four-wing chaotic systems via sliding mode control, *International Journal of Automation and Computing*, vol. 9(3), pp. 274-279 (2012).
63. V. Sundarapandian and R. Karthikeyan, Anti-synchronization of hyperchaotic Lorenz and hyperchaotic Chen systems by adaptive control, *International Journal of System Signal Control and Engineering Applications*, vol. 4, pp. 18-25 (2011).
64. V. Sundarapandian and R. Karthikeyan, Anti-synchronization of Lu and Pan chaotic systems by adaptive nonlinear control, *International Journal of Soft Computing*, vol. 6, pp. 111-118 (2011).
65. V. Sundarapandian and R. Karthikeyan, Adaptive anti-synchronization of uncertain Tigan and Li systems, *Journal of Engineering and Applied Sciences*, vol. 7, pp. 45-52 (2012).
66. S. Vaidyanathan and S. Pakiriswamy, Generalized projective synchronization of Sundarapandian chaotic systems by adaptive control, *International Journal of Control Theory and Applications*, vol. 6(2), pp. 153-163, (2013).
67. S. Vaidyanathan, Anti-synchronization of Sprott-L and Sprott-M chaotic systems via adaptive control, *International Journal of Control Theory and Applications*, vol. 5(1), pp. 41-59 (2012).
68. P. Sarasu and V. Sundarapandian, Adaptive controller design for the generalized projective synchronization of 4-scroll systems, *International Journal of Systems Signal Control and Engineering Application*, vol. 5(2), pp. 21-30, (2012).
69. P. Sarasu and V. Sundarapandian, Generalized projective synchronization of two-scroll systems via adaptive control, *International Journal of Soft Computing*, vol. 7(4), pp. 146-156, (2012).
70. S. Rasappan and S. Vaidyanathan, Global chaos synchronization of WINDMI and Coulet chaotic systems using adaptive backstepping control design, *Kyungpook Mathematical Journal*, vol. 54(1), pp. 293-320 (2014).
71. H.K. Khalil, *Nonlinear System*, 3rd ed., Prentice Hall, New Jersey, USA (2002).
72. I.M. Kyprianidis, Ch.K. Volos, S.G. Stavrinides, I.N. Stouboulos, A. N. Anagnostopoulos, On-off intermittent synchronization between two bidirectional coupled double scroll circuits, *Commun. Nonlinear Sc. Numer. Simulat.*, vol. 15, pp. 2192-2200 (2010).
73. J.C. Sprott, A proposed standard for the publication of new chaotic systems, *Int. J. Bif. Chaos*, vol. 21, pp. 2391-2394 (2011).
74. S. Banerjee, Chaos synchronization and cryptography for secure communications: Applications for encryption, IGI Global, U.S.A. (2010).
75. S. Boccaletti, J. Kurths, G. Osipov, D.L. Valladares, and C.S. Zhou, The synchronization of chaotic systems, *Physics Reports*, vol. 366, pp. 1-101 (2002).
76. M.E. Yalcin, J.A.K. Suykens and J. Vandewalle, True random bit generator from a double-scroll attractor, *IEEE Trans. Circuits Sys. I: Regular Papers*, vol. 51, pp. 1395-1404 (2004).
77. Ch. K. Volos, I. M. Kyprianidis, and I. N. Stouboulos, Motion control of robots using a chaotic truly random bits generator, *Journal of Engineering Science and Technology Review*, vol 5(2), pp. 6-11 (2012).
78. Ch. K. Volos, I. M. Kyprianidis, and I. N. Stouboulos, A chaotic path planning generator for autonomous mobile robots, *Robotics and Autonomous Systems*, vol. 60, pp. 651-656 (2012).
79. Ch. K. Volos, I. M. Kyprianidis, and I. N. Stouboulos, Image encryption process based on chaotic synchronization phenomena, *Signal Processing*, vol. 93, pp. 1328-1340 (2013).
80. Ch. K. Volos, I. M. Kyprianidis, and I. N. Stouboulos, Experimental investigation on coverage performance of a chaotic autonomous mobile robot, *Robotics and Autonomous Systems*, vol. 61(12), pp. 1314-1322 (2013).